

Optical Engineering

OpticalEngineering.SPIEDigitalLibrary.org

Inertial sensor-based multiloop control of fast steering mirror for line of sight stabilization

Jing Tian
Wenshu Yang
Zhenming Peng
Tao Tang

Inertial sensor-based multiloop control of fast steering mirror for line of sight stabilization

Jing Tian,^{a,b,c,d,*} Wenshu Yang,^{a,c} Zhenming Peng,^b and Tao Tang^{a,c}

^aInstitute of Optics and Electronics, Chinese Academy of Science, No. 1 Guangdian Road, Wenxin town, Shuangliu county, Chengdu 610209, China

^bUniversity of Electronic Science and Technology of China, School of Opto-Electronic Information, No. 4, Section 2, Jianshe North Road, Chengdu 610054, China

^cChinese Academy of Sciences, Key Laboratory of Optical Engineering, Chengdu 610209, China

^dUniversity of Chinese Academy of Sciences, Beijing 100039, China

Abstract. In the charge-coupled device (CCD)-based tracking control system of fast steering mirrors (FSMs), high control bandwidth is the most effective method to enhance closed-loop performance, which, however, usually suffers a great deal from time delay induced by a low CCD sampling rate. Moreover, mechanical resonances also limit high control bandwidth. Therefore, a tentative approach to implementing a CCD-based tracking control system for an FSM with inertial sensor-based cascade feedback is proposed, which is made up of acceleration feedback, velocity feedback, and position feedback. Accelerometers and gyroscopes are all the inertial sensors, sensing vibrations induced by platforms, in turn, which can contribute to disturbance supersession. In theory, the acceleration open-loop frequency response of the FSM includes a quadratic differential, and it is very difficult to compensate a quadratic differential with a double-integral algorithm. A lag controller is used to solve this problem and accomplish acceleration closed-loop control. The disturbance suppression of the proposed method is the product of the error attenuation of the acceleration loop, the velocity loop, and the position loop. Extensive experimental results show that the improved control mode can effectively enhance the error attenuation performance of the line of sight (LOS) for the CCD-based tracking control system. © The Authors. Published by SPIE under a Creative Commons Attribution 3.0 Unported License. Distribution or reproduction of this work in whole or in part requires full attribution of the original publication, including its DOI. [DOI: [10.1117/1.OE.55.11.111602](https://doi.org/10.1117/1.OE.55.11.111602)]

Keywords: acceleration feedback control; fast steering mirror; multiloop control; light of sight stabilization; inertial sensor.

Paper 151785SS received Dec. 17, 2015; accepted for publication May 4, 2016; published online Jul. 21, 2016.

1 Introduction

Fast steering mirror (FSM) control systems are extensively applied to optoelectronic tracking equipment, which is increasingly mounted on airplanes, vessels, vehicles, and other moving platforms. In the classical FSM control system, the inertial velocity sensors (such as gyroscopes) and charge-coupled device (CCD) are generally used to implement a dual closed-loop control to stabilize line of sight (LOS).¹⁻⁴ High closed-loop control bandwidth facilitates good closed-loop performance. However, the control bandwidth is limited mainly by sensors and mechanical resonances.

Acceleration feedback control (AFC) is a kind of high-precision robust control. It was proposed by Studenny and Belanger,⁵ and its application in mechanical arm control was reported in a paper in 1991.⁶ de Jager⁷ studied the application of AFC in tracking control. Application research of acceleration feedback performed in torque control and direct-driven mechanical arms shows that AFC is a highly effective technique.^{8,9} In the above research, the actuator was the rotary motor. In theory, the acceleration open-loop transfer function of this system driven by the rotary motor characterizes a low-pass filter. However, the actuators used in the FSM control system are voice coil motors, and the acceleration open-loop transfer function includes a quadratic differential. In recent years, some scholars have used accelerometers and focal plane arrays (FPAs) to implement

closed-loop control of the FSM.¹⁰⁻¹² Accelerometers have poor low-frequency response ability; meanwhile, there exists a large drift in the double integral data of accelerometers, which should be corrected with the FPA. Therefore, it is difficult to use only accelerometers in FSM control systems. The position information obtained from double integration of accelerometers fused with FPA data was used to achieve position loop control.^{10,11} Strictly speaking, it is a single-loop position control. Tang¹² combined a CCD and accelerometers to implement dual closed-loop control with acceleration and position. In order to avoid the saturation of double integration, the acceleration controller was designed as a band-pass filter. Therefore, there is still a quadratic differential effect within the low-frequency range, and the disturbance suppression of the FSM control system for low-frequency vibration is insufficient.

In this paper, a three-closed-loop control model (acceleration feedback, velocity feedback, and position feedback) is proposed to enhance the closed-loop performance of the FSM control system, and a lag controller is used to accomplish acceleration closed-loop control. The velocity controller can be designed as a PI type controller, because the velocity open-loop response with AFC exhibits mainly an integrator. The disturbance suppression of the proposed method is the product of the error attenuation of the acceleration loop, the velocity loop, and the position loop. This paper is organized as follows. Section 2 presents a detailed introduction to the control model of the FSM, mainly describing the CCD-based control structure and the implementation of AFC. Section 3 discusses and analyzes system

*Address all correspondence to: Jing Tian, E-mail: abb1978@163.com

performance. Section 4 sets up experiments to verify this method. Concluding remarks are presented in Sec. 5.

2 Fast Steering Mirror Control System Model

The configuration of the FSM control system is shown in Fig. 1. The sensors include accelerometers, gyroscopes, and a CCD. The controller is used to implement the control algorithm. The driver actuates the voice coil motors to achieve stabilization control of the FSM. The light source is used to simulate the target of the CCD.

The mechanical part of the FSM is a typical resonance element, while its electrical part is a typical first-order inertial element. Therefore, the FSM position open-loop response can be expressed as follows:

$$G_p(s) = \frac{\theta(s)}{U(s)} = \frac{K}{\frac{s^2}{\omega_n^2} + \frac{2\xi}{\omega_n}s + 1} \cdot \frac{1}{T_e s + 1}. \quad (1)$$

The open-loop natural frequency of FSMs, ω_n , is approximately above several Hz, and the damping factor ξ is much smaller than 1.¹³

The traditional FSM control system without AFC is shown in Fig. 2.

When the velocity and position closed-loops are achieved, the disturbance suppression of the control system is the

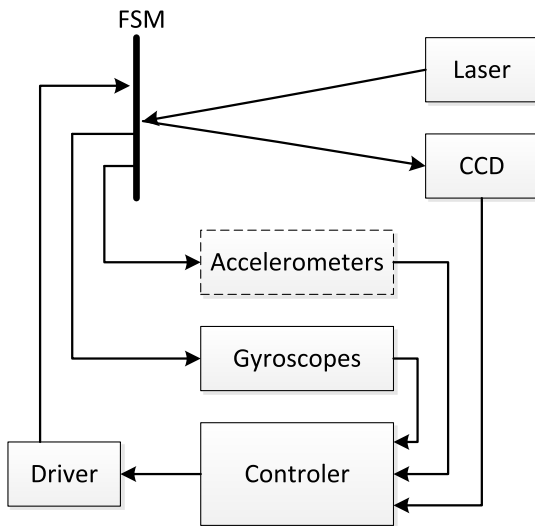


Fig. 1 Configuration of the FSM control system.

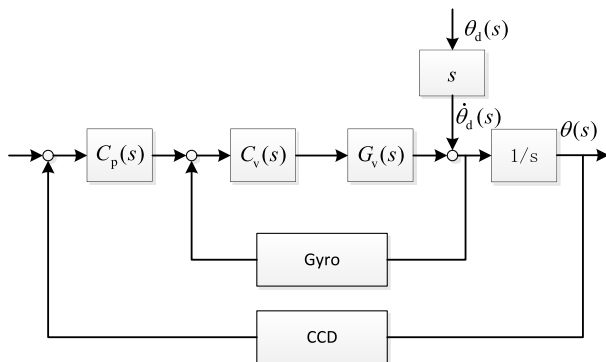


Fig. 2 Traditional FSM control system.

product of the error attenuation of the velocity loop and that of the position loop.

$$E''_{\theta} = \frac{\theta(s)}{\theta_d(s)} = \frac{1}{1 + G_v C_v + \frac{1}{s} G_v C_v C_p} = \frac{1}{1 + G_v C_v} \cdot \frac{1}{1 + \frac{1}{s} \frac{G_v C_v}{1 + G_v C_v} C_p} \approx \frac{1}{1 + G_v C_v} \cdot \frac{1}{1 + \frac{1}{s} C_p}. \quad (2)$$

In order to improve the overall disturbance suppression, it is necessary to enhance the error attenuation performance of the velocity loop and the position loop by increasing their closed-loop bandwidth. The error attenuation performance of the position loop depends on the LOS error from the CCD sensor. Because of the time delay and low sample of the CCD, the performance of the position loop is certainly restricted. The closed-loop bandwidth of the velocity loop is affected mainly by mechanical resonance and the gyroscope's bandwidth.

Therefore, the AFC is introduced to further enhance the closed-loop performance of the FSM control system. The FSM acceleration open-loop response $G_a(s)$ has a higher quadratic differential than $G_p(s)$, which is depicted in Eq. (1).

$$G_a(s) = \frac{\ddot{\theta}(s)}{U(s)} = \frac{K}{\frac{s^2}{\omega_n^2} + \frac{2\xi}{\omega_n}s + 1} \cdot \frac{s^2}{T_e s + 1}. \quad (3)$$

The ideal acceleration controller can be designed as the inverse transfer function $G_a(s)$. In order to increase the system gain, an integrator should be added. The ideal acceleration controller can be presented as follows:

$$C_a(s) = K_a \cdot \frac{1}{s} \cdot \frac{\frac{s^2}{\omega_n^2} + \frac{2\xi}{\omega_n}s + 1}{K} \cdot \frac{T_e s + 1}{s^2}. \quad (4)$$

Since the controller is a complete pole-zero cancellation, the acceleration closed-loop transfer function may theoretically have high bandwidth. However, there are some disadvantages for the controller: saturated double integration, worse disturbance suppression, and stability of the system induced by the inaccurate control function, which is derived from inaccurate fitting of $G_a(s)$ due to the noise and measuring error of accelerometers. To avoid the above deficiencies, the acceleration controller C'_a is designed as

$$C'_a = \frac{K_a}{s} \cdot \frac{T_e s + 1}{T_1 s + 1}, \quad (5)$$

where $T_e s + 1$ is used to compensate phase loss. The integrator is used to partly compensate the quadratic differential. The lag element with a small time constant is used to filter the high-frequency noise. The designed value of T_1 should be smaller than 0.01; otherwise, the bandwidth of the control system will be too low. The closed-loop acceleration transfer function is expressed as follows:

$$\begin{aligned}
 G_{a_closed} &= \frac{\frac{K_a K s}{(T_1 s + 1) \left(\frac{s^2}{\omega_n^2} + \frac{2\xi}{\omega_n} s + 1 \right)}}{1 + \frac{K_a K s}{(T_1 s + 1) \left(\frac{s^2}{\omega_n^2} + \frac{2\xi}{\omega_n} s + 1 \right)}} \\
 &= \frac{K_a K s}{(T_1 s + 1) \left(\frac{s^2}{\omega_n^2} + \frac{2\xi}{\omega_n} s + 1 \right) + K_a K s} \\
 &= \frac{K_a K s}{\frac{T_1}{\omega_n^2} s^3 + \left(\frac{1}{\omega_n^2} + \frac{2\xi T_1}{\omega_n} \right) s^2 + \left(K_a K + T_1 + \frac{2\xi}{\omega_n} \right) s + 1}.
 \end{aligned} \tag{6}$$

This equation is similar to a bandpass filter. G_{a_closed} approaches zero at high frequencies. On the basis of analyzing of Eqs. (1) and (6), the denominator of Eq. (6) can be simplified to $K_a K s + 1$ at low frequencies. Then G_{a_closed} can be simplified as follows:

$$\begin{aligned}
 G'_{a_closed} &= \frac{K_a K s}{\frac{T_1}{\omega_n^2} s^3 + \left(\frac{1}{\omega_n^2} + \frac{2\xi T_1}{\omega_n} \right) s^2 + \left(K_a K + T_1 + \frac{2\xi}{\omega_n} \right) s + 1} \\
 &\approx \frac{K_a K s}{\left(K_a K + T_1 + \frac{2\xi}{\omega_n} \right) s + 1} \approx \frac{K_a K s}{K_a K s + 1}.
 \end{aligned} \tag{7}$$

It is clear that the acceleration controller has a high gain K_a ; thus, the value of $K_a K s$ is large enough to keep certain gain of the closed loop at low frequency, which is smaller than that of the ideal closed loop. The analysis will be verified by later experiments.

The velocity open-loop response of the FSM with AFC at low frequency is depicted as

$$\begin{aligned}
 G_{v_a_closed} &= \frac{1}{s} G_{a_closed} \\
 &= \frac{K_a K}{(T_1 s + 1) \left(\frac{s^2}{\omega_n^2} + \frac{2\xi}{\omega_n} s + 1 \right) + K_a K s} \\
 &\approx \frac{K_a K}{K_a K s + 1}.
 \end{aligned} \tag{8}$$

Therefore, the traditional PI controller can meet the velocity closed-loop control, which is designed as

$$C_v = K_{v1} \cdot \frac{K_{v2} s + 1}{s}. \tag{9}$$

The position open-loop response of the FSM with acceleration and velocity feedback control can be measured and depicted as follows:

$$G_p = \frac{K_p}{s(T_{p1} s + 1) \left(\frac{s^2}{\omega_n^2} + \frac{2\xi}{\omega_n} s + 1 \right)} e^{-T_{p2} s}. \tag{10}$$

This can be simplified as follows at low frequencies:

$$G'_p \approx \frac{K'_p}{s(T_{p1} s + 1)} e^{-T_{p2} s}. \tag{11}$$

Therefore, the traditional PI controller can meet the position closed-loop control, which is depicted as

$$C_p = K_{p1} \cdot \frac{K_{p2} s + 1}{s}. \tag{12}$$

3 Analyzing Multiloop Control

The multiloop control structure of the FSM is shown in Fig. 3. For the FSM control system, the objective is to improve disturbance suppression performance.

Where $G_a(s)$ is the acceleration open-loop transfer function, $C_a(s)$ is the acceleration controller, $C_v(s)$ is the velocity controller, $C_p(s)$ is the position controller, $\theta(s)$ is the angular velocity output, $\theta_d(s)$ is the disturbance angle, and $\ddot{\theta}_d(s)$ is the disturbance acceleration.

The disturbance suppression of the FSM with three closed loops can be expressed as follows:

$$\begin{aligned}
 E_\theta &= \frac{\theta(s)}{\theta_d(s)} = \frac{1}{1 + G_a C_a + \frac{1}{s} G_a C_a C_v + \frac{1}{s^2} G_a C_a C_v C_p} \\
 &= \frac{1}{1 + G_a C_a} \cdot \frac{1}{1 + \frac{1}{s} \frac{G_a C_a}{1 + G_a C_a} C_v} \cdot \frac{1}{1 + \frac{1}{s} \frac{\frac{1}{s} G_a C_a C_v}{1 + \frac{1}{s} \frac{G_a C_a}{1 + G_a C_a} C_v} C_p} \\
 &\approx \frac{1}{1 + G_a C_a} \cdot \frac{1}{1 + \frac{1}{s} C_v} \cdot \frac{1}{1 + \frac{1}{s} C_p},
 \end{aligned} \tag{13}$$

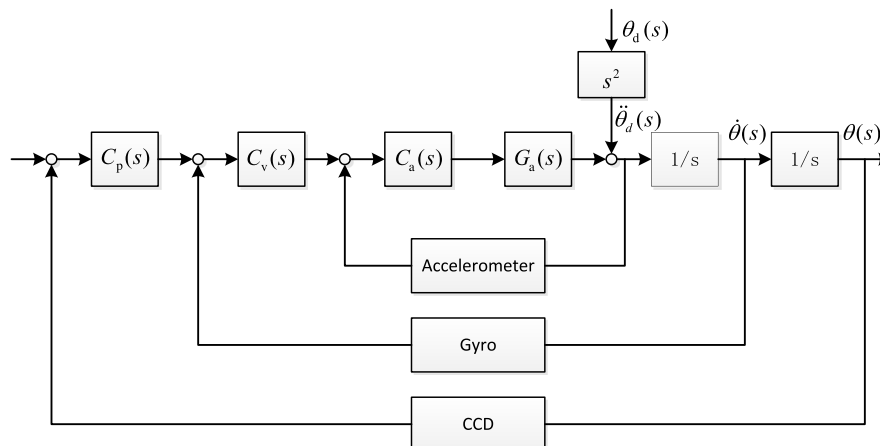


Fig. 3 Stability control structure of multiple closed loops.

where

$$\frac{\frac{1}{s} \frac{G_a C_a}{1+G_a C_a} C_v}{1 + \frac{1}{s} \frac{G_a C_a}{1+G_a C_a} C_v} \approx 1, \quad \frac{G_a C_a}{1 + G_a C_a} \approx 1. \quad (14)$$

According to Eqs. (2) and (13), the disturbance suppression is theoretically improved by about 20 db after the acceleration closed-loop is added. In practice, the disturbance suppression can be increased by more than 20 db at certain frequencies because the AFC improves the velocity open-loop response of the FSM and provides a good object for velocity feedback control, which will be verified by a later experiment. Therefore, the disturbance suppression of the system is nearly equal to the product of the individual suppression of the three closed loops at low frequencies within the acceleration closed-loop bandwidth.

For the velocity open-loop transfer function without AFC, the function sensitivity is equal to 1. With AFC, the function sensitivity becomes

$$S_{G_a}^{\theta} = \frac{\left(\frac{(G_a + \Delta G_a) C_a C_v}{1 + (G_a + \Delta G_a) C_a} \cdot \frac{1}{s} - \frac{G_a C_a C_v}{1 + G_a C_a} \cdot \frac{1}{s} \right) / \left(\frac{G_a C_a C_v}{1 + G_a C_a} \cdot \frac{1}{s} \right)}{\Delta G_a / G_a} \approx \frac{G_a C_a}{(1 + G_a C_a)^2} \approx \frac{1}{1 + G_a C_a}. \quad (15)$$

Provided that the gain of the acceleration controller is large enough, $S_{G_a}^{\theta}$ is far less than 1. When the relevant structures and parameters of the system change greatly, the robustness of the velocity closed-loop system with AFC will not be affected. The gain of the acceleration controller actually exceeds 100, so the system is robust.

4 Experimental Verification

The FSM control system is a two-axis system. This experiment aims at one axis due to the symmetry of the two axes. The experimental setup is shown in Fig. 4, which includes a disturbance platform, a stabilized platform, a laser light, and an image processing system (CCD). The two platforms are driven by the voice coil motors. The disturbance platform simulates the disturbance of the carrier, on which the fiber-optic gyroscope1 (Gyro1) and the eddy current displacement sensor are used for disturbance measurement; Gyro1 is used to measure the disturbance angular velocity of the platform, and the eddy is used to measure the disturbance angle of the platform. The stabilized platform is mounted on the disturbance platform. The microelectromechanical system (MEMS) linear accelerometers mounted on the stabilized platform are used to measure the angular acceleration of the platform. Gyro2 is used to measure the angular velocity of the stabilized platform. The light source is used to simulate the target, and the mirror reflects the laser light into the CCD, which detects the LOS of the stabilized platform and provides LOS error (Fig. 4).

The MEMS accelerometer bandwidth exceeds 1000 Hz, and the angular acceleration can be obtained from two line accelerometers.¹⁰ The bandwidth of the fiberoptic gyroscope exceeds 500 Hz.

The total disturbance suppression of the control system including passive and active disturbance suppression is measured with the CCD and eddy sensors of the disturbance

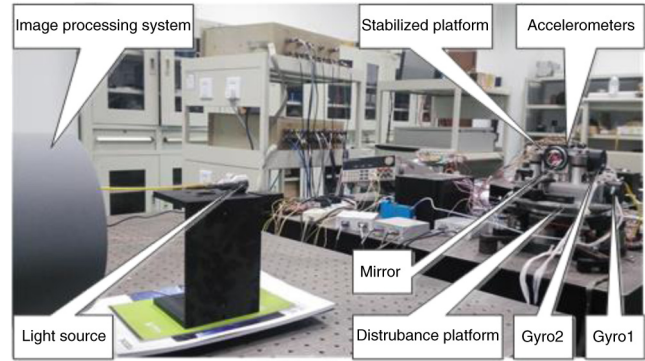


Fig. 4 Experimental apparatus.

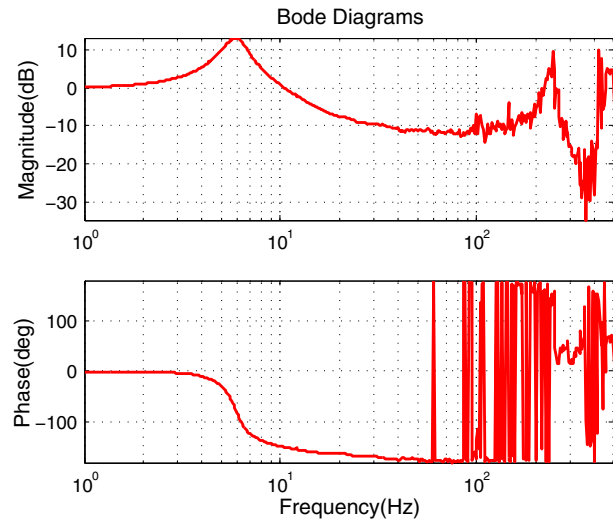


Fig. 5 Passive disturbance suppression characteristics when control system of FSM is open.

platform when the disturbance platform simulates the disturbance of the carrier and the control system of the stabilized platform is closed. Passive disturbance suppression is measured when the disturbance platform simulates the disturbance of the carrier and the control system of the stabilized platform is open. Active disturbance is measured on the condition that the disturbance platform stays static. The frequency of the disturbance simulated by the disturbance platform is from 1 to 500 Hz.

Figure 5 shows the passive disturbance suppression of the FSM. From Eq. (3), the open-loop acceleration characteristic of the FSM at low frequency is similar to a second-order integrator. Figure 6 shows the open-loop and closed-loop acceleration response. The acceleration closed-loop bandwidth exceeds 700 Hz and the closed-loop acceleration response includes a small differential effect at low frequency, which is depicted in Eq. (7).

The closed-loop bandwidth of the single velocity loop is about 200 Hz in Fig. 7, which is similar to that of the velocity loop with AFC. Therefore, the AFC cannot produce any adverse effect on the velocity loop.

Figure 8 shows the CCD closed-loop response of the velocity closed-loop FSM without AFC and with AFC. The closed-loop bandwidths of two kinds of systems all reach about 40 Hz. The static position error of the system

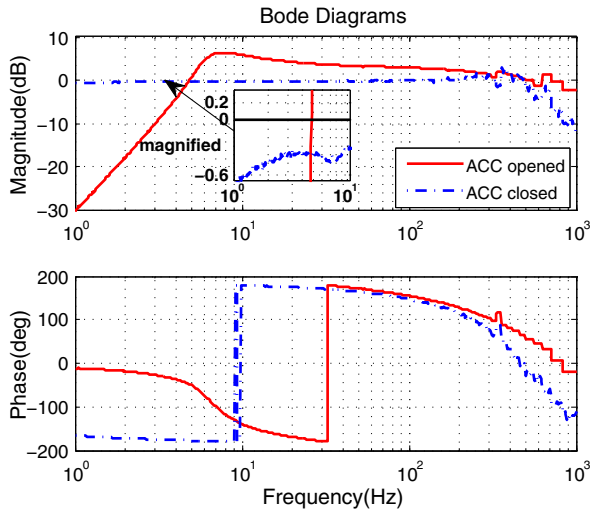


Fig. 6 FSM acceleration response.

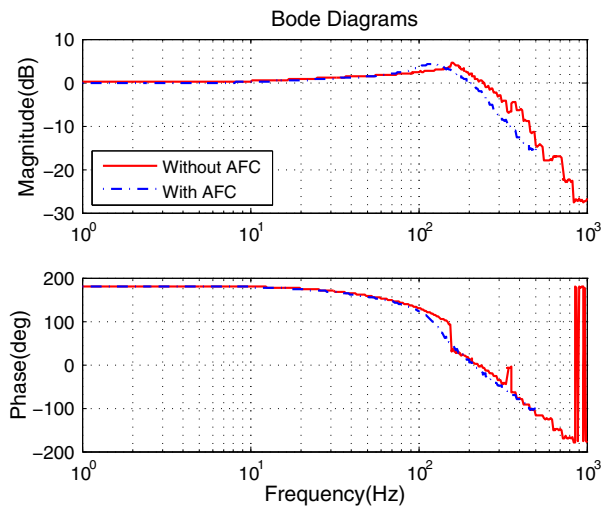


Fig. 7 Velocity closed-loop response.

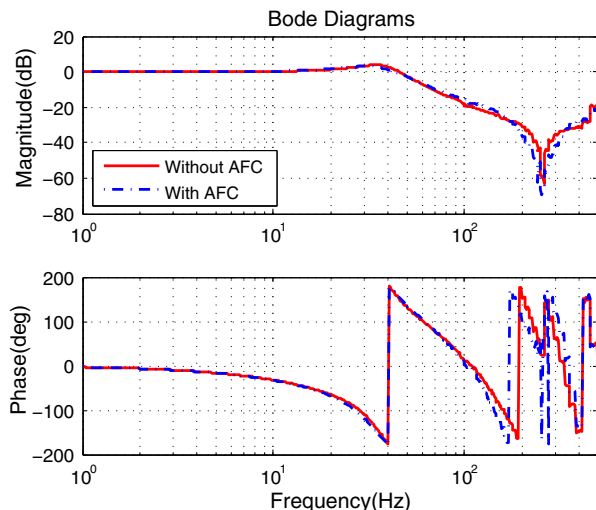


Fig. 8 CCD closed-loop response.

without AFC is ~ 0.113 pixels, while the static position error with AFC is 0.116 pixels, which is a little larger than that without AFC. The additional error comes from electronic and sensor noise.

The rejection characteristics of the three control loops are shown in Fig. 9. The rejection bandwidth of the acceleration loop is about 200 Hz, and the others are 90 and 20 Hz.

The total disturbance suppression characteristics of the FSM control system with the CCD and gyroscope feedback are shown in Fig. 10. The disturbance suppression with AFC is much better than that without AFC.

The total disturbance suppression of the FSM control system is shown in Table 1.

It is shown in Fig. 10 and Table 1 that with AFC, the disturbance suppression of the FSM control system is improved by about 20 dB below the frequency of 10 Hz, and it is enhanced by more than 20 dB from 10 to 20 Hz. The experimental result accords with the above analysis of Eq. (2) and (13). The disturbance suppression with AFC becomes a little weaker than that without AFC at about 200 Hz because of the AFC amplification.

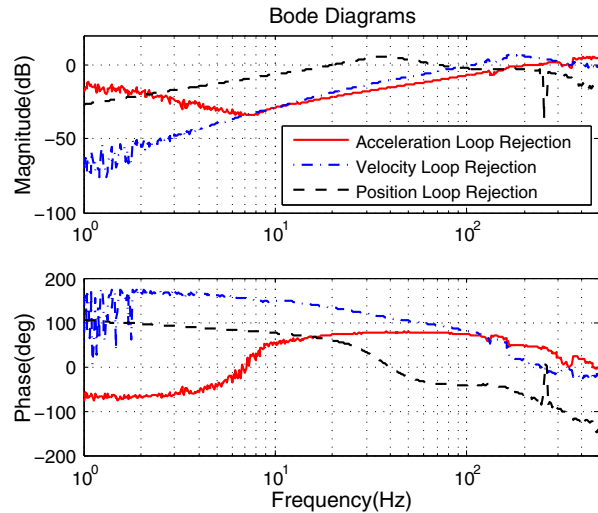


Fig. 9 Rejection characteristics of the three kinds of control loops.

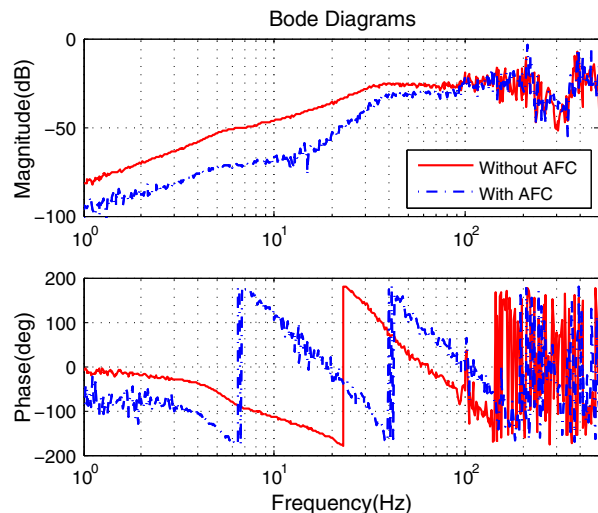


Fig. 10 Disturbance suppression characteristics.

Table 1 Comparison between disturbance suppressions of two kinds of FSM control systems.

Frequency (Hz)	Without AFC (dB)	With AFC (dB)
1	-81.39	-103.5
10	-46.39	-67.5
15	-41.18	-64.53
20	-35.77	-53.01
40	-25.57	-31.33
100	-21.97	-21.85

5 Conclusion

Acceleration feedback was introduced to enhance the stabilization performance of the FSM control system. The modeling of FSM acceleration via linear accelerometers was discussed from the viewpoint of its practical implementation. The simplification for implementing AFC in the FSM control system was presented mainly in terms of closed-loop stability and error attenuation. The algebraic expression shows that AFC can effectively enhance the robustness of the closed-loop control system, and the experimental results showed that acceleration feedback can effectively enhance the stabilization performance of the closed-loop control system.

Future work will concentrate on reducing the cost of the FSM control system in the condition of good closed-loop performance. The use of only accelerometers may be an effective method, which will be our next work. Furthermore, excellent hardware is also important for the FSM control system.

Acknowledgments

The authors sincerely thank the anonymous reviewers for their valuable comments and suggestions on the paper.

References

1. M. F. Luniewicz et al., "Comparison of wide-band inertial line of sight stabilization reference mechanizations," *Proc. SPIE* **1697**, 378 (1992).

2. R. Walter et al., "Stabilized inertial measurement system (SIMS)," *Proc. SPIE* **4724**, 57 (2002).
3. J. M. Hilkert, "Development of mirror stabilization line-of-sight rate equations for an un-conventional sensor-to-gimbal orientation," *Proc. SPIE* **7338**, 733803 (2009).
4. J. M. Hilkert, "A comparison of inertial line-of-sight stabilization techniques using mirrors," *Proc. SPIE* **5430**, 13 (2004).
5. J. Studenny and P. R. Belanger, "Robot manipulator control by acceleration feedback," in *Proc. of 23rd IEEE Conf. on Decision and Control* (1984).
6. J. Studenny et al., "A digital implementation of the acceleration feedback control law on a PUMA 560 manipulator," in *Proc. of the 30th IEEE Conf. on Decision and Control*, Vol. 3, pp. 2639–2648 (1991).
7. B. de Jager, "Acceleration assisted tracking control," *J. IEEE Control Syst.* **14**(5), 20–27 (1994).
8. H. Jianda et al., "Joint acceleration feedback control for direct-drive robot decoupling," *J. Acta Autom. Sin.* **26**(3), 289–295 (2000).
9. H. Jianda et al., *Mobile Robot System: Modeling, Estimation and Control*, Science Press, Beijing, China (2001).
10. S. Lee et al., "Accelerometer-assisted tracking and pointing for deep space optical communications," in *Proc. of Conf. on Aerospace*, Vol. 3, pp. 3/1559–3/1564 (2001).
11. G. G. Ortiz et al., "Functional demonstration of accelerometer-assisted beacon tracking," *Proc. SPIE* **4272**, 112 (2001).
12. T. Tang et al., "Acceleration feedback of a CCD-based tracking loop for fast steering mirror," *Opt. Eng.* **48**(1), 013001 (2009).
13. R. W. Cochran and R. H. Vassar, "Fast steering mirrors in optical control systems," *Proc. SPIE* **1303**, 7 (1990).

Jing Tian received his MS degree in 2007 from Xi'an Jiaotong University. He joined the Institute of Optics and Electronics, Chinese Academy of Sciences, where he is currently an associate professor and pursuing his PhD. His research interests include control-based sensors, inertial stabilization, and optical signal processing.

Wenshu Yang is with the Institute of Optics and Electronics. She is a professor and doctor director in the Institute of Optics and Electronics. Currently, her research interests include technology of beam control and optical engineering.

Zhenming Peng is with the School of Opto-Electronic Information, University of Electronic Science and Technology of China. He is a professor and doctor director in the Institute of Optics and Electronics. Currently, his research interests include technology of image processing and optical engineering.

Tao Tang received his PhD in 2009 from the Institute of Optics and Electronics, Chinese Academy of Sciences. He joined this institute after his graduation, and he is currently an associate professor. His research interests include control-based sensors, FSM control, adaptive control, and inertial stabilization.